

Structural, dynamical, and electronic properties of CaCuO_2

Bal K. Agrawal and Savitri Agrawal

Physics Department, Allahabad University, Allahabad 211002, India

(Received 23 March 1993)

The scalar relativistic version of an accurate first-principles full-potential self-consistent linearized muffin-tin-orbital (LMTO) method has been employed for describing the physical properties of the parent system of the high- T_c oxide superconductors, i.e., CaCuO_2 . The presently employed modified version of the LMTO method is quite fast and extends the usual LMTO-ASA (atomic-sphere approximation) method in the sense that it permits a completely general shape of the potential and the charge density and is also capable of treating distorted lattice structures accurately. The calculated values of the lattice parameters of pure CaCuO_2 lie within 3% of the experimentally measured values for the Sr-doped system $\text{Ca}_{1.86}\text{Sr}_{0.14}\text{CuO}_2$. The computed electronic structures and the density of states are quite similar to those of the other oxide superconductors, except for their three-dimensional character because of the presence of strong coupling between the closely spaced CuO_2 layers. The calculated frequencies for the $\mathbf{k}=0$ frozen phonons for undoped CaCuO_2 are quite close to the measured data for Sr-doped CaCuO_2 .

I. INTRODUCTION

In the last decade it has been observed that structural and lattice-dynamical properties can be determined *ab initio* with reliable accuracy if one can calculate the electronic energy of the solid as a function of the atomic positions using the usual density-functional theory.

Recently, the linear muffin-tin orbital (LMTO) method has drawn much attention towards its application to the study of the electronic structure of molecules as well as of crystalline solids. The method has several advantages: (i) Only a minimal basis set is required in the method thus it enables its application to large unit cells with high efficiency. (ii) The method treats all the elements of the Periodic Table in a similar manner. Thus, the atoms with a large number of core states and metals having prominently *d* or *f* character can be treated easily. (iii) As the augmentation procedure generates the correct shape of the wave function near the nuclei, it is quite accurate. (iv) The use of atom-centered basis functions belonging to the different values of the angular momentum in the method helps one to have a quite clear physical picture.

Usually in the application of the standard LMTO method, an atomic-sphere approximation (ASA) is used to make it efficient. However, this LMTO-ASA method suffers with several disadvantages. (i) It neglects the symmetry-breaking terms by discarding the nonspherical parts of the electron density. (ii) The method discards the interstitial region by replacing the muffin-tin spheres by the space-filling Wigner spheres. (iii) It uses spherical Hankel functions with vanishing kinetic energy only.

It has been noted that quite reliable results could be attained by employing a LMTO basis set if all the potential terms are determined accurately. For this, the sizes of the atomic spheres are shrunk to make them nonoverlapping. The potential matrix elements then split into two parts: one contribution coming from the atomic spheres and the other one from the complicated interstitial region. The first part, i.e., the atomic sphere one, is easy to evaluate by expanding it in terms of the usual spherical

harmonics. On the other hand, the evaluation of the interstitial contribution is quite difficult and very time consuming if done by standard techniques.

Efforts have been made to find an efficient and quick way to determine the interstitial contribution. In the method used in the present work, the interstitial quantities were expanded in terms of the spherical Hankel functions. The involved three-center integrals were expressed as the linear combination of the two center integrals by numerical means. These two-center integrals involving Hankel functions can easily be evaluated analytically. The method does not employ the plane waves and is thus applicable to the periodic as well as the nonperiodic systems which are so often need to be treated especially when there occur impurities, defects, and lattice distortions or atomic relaxations.

The present LMTO method is seen to give the electronic structure, cohesive energy, lattice constants, elastic constants, phonon frequencies, mode Grüneisen and strain parameters for simple systems like Si, C, etc.^{1,2} Very recently, the method has also been successfully applied to the III-V and II-VI semiconducting compounds like AlAs, CdS, GaSb, ZnSe, ZnTe, ZnS (Ref. 3), etc. The influence of the structural relaxation of the atoms on the valence-band offset at the lattice matched interfaces of the II-VI and III-V semiconductors ZnTe/GaSb(110) and the lattice mismatched interface ZnS/ZnSe(001) have been investigated.⁴

In most of the high- T_c oxide superconductors forming the homologous series $A_{1(2)}B_2Ca_{n-1}Cu_nO_{2n+3(4)}$ with $A = \text{Tl}$ or Bi and $B = \text{Ba}$ or Sr , the n - (CuO_2) layers are interleaved with the $(n-1)$ calcium layers and they are separated by $Ab\text{O}_2$ units with NaCl structure. The transition temperature T_c increases with n : for Bi and bilayer thallium (Tl_2) compounds up to $n=3$ and for monolayer thallium (Tl) compounds up to $n=4$. The highest value of T_c attained so far is 125 K for the Tl phases.⁵

A compound CaCuO_2 is obtained if the number of CuO_2 planes is allowed to increase indefinitely ($n \rightarrow \infty$). Thus, CaCuO_2 is the infinite number of CuO_2 layers limit

of the above superconductors and is seen to be insulating.⁶ T_c might increase with n .

In the crystal structure of the stable $\text{Ca}_{1-x}\text{Sr}_x\text{CuO}_2$, only Ca or Sr ions separate CuO_2 layers. It is a highly defective structure, a perovskite with a third of the oxygen positions vacant. The copper is bonded to only four coplanar oxygen ions and the connecting layer units $Ab\text{O}_2$ present in the usual $A_2B_2\text{Ca}_{n-1}\text{Cu}_n\text{O}_{2n+4}$ systems are totally absent in CaCuO_2 . The connecting units $Ab\text{O}_2$ are likely to modify the electrical properties of the high- T_c superconductors by the consequent changes to the copper environment and possibly its valence.

In the $A_2B_2\text{Ca}_{n-1}\text{Cu}_n\text{O}_{2n+4}$ superconductors or in the $\text{YBa}_2\text{Cu}_3\text{O}_7$ material, because of the presence of $Ab\text{O}_2$ unit layers, the copper ions in addition to their four coplanar oxygen ions have one more oxygen ion lying along the c axis forming a square pyramid of five oxygen atoms. In La_2CuO_4 , the Cu ion has six oxygen ions forming an octahedral with four short and two long (stretched ones along the c axis) bonds. Nonoccurrence of superconductivity is possible because most of the copper-oxide superconductors contain layers of Jahn-Teller distorted copper ions bonded to either five oxygens or six oxygens. One also remembers that, whereas Sr or Ba doping of La_2CuO_4 yields superconductors, similar doping has been seen to be ineffective in Eu_2CuO_4 in which CuO_2 layers and Cu coordination are similar to $\text{Ca}_{0.86}\text{Sr}_{0.14}\text{CuO}_2$. The $n = \infty$ material appears to be more difficult to dope. However, more recently $(\text{CaSr})\text{CuO}_2$ has been doped successfully and an electron-type superconductivity has been seen.⁷

In high- T_c superconductors, an idea of a mixed valence of $\text{Cu}^{2+}/\text{Cu}^{3+}$ has been favored. As some Cu^{3+} has been assumed essential for superconductivity, there are propositions that Cu^{3+} either compensates for incomplete occupancy of the A or B sites or results from electron transfer from copper bands to thallium $6s$ or bismuth $6p$ bands. On the other hand, in the CaCuO_2 material the absence of $AB\text{O}_2$ layers eliminates the possibility of the occurrence of both mechanisms and for this strictly Cu^{2+} compound, electron correlation effects are likely to incur localized spins, antiferromagnetic exchange, and semiconducting behavior. In practice, the $n = \infty$ structure is not formed with only a Ca ion on the A site, a material with some Ca substitution by Sr, $\text{Ca}_{0.86}\text{Sr}_{0.14}\text{CuO}_2$, has been prepared. The Sr mixed compound is seen to be a narrow-band semiconductor.

Earlier, some efforts in the direction of the calculation of the electronic structure of CaCuO_2 have been made. Mattheiss and Hamann⁸ and Singh *et al.*⁹ have employed the linear-augmented-plane-wave (LAPW) method whereas Koroton and Anisimov¹⁰ have employed the LMTO-ASA method. The limitations of the atom-sphere approximation version of the LMTO have already been discussed above.

We have employed a scalar relativistic version of an accurate and fast first-principles full potential self-consistent LMTO method for the ideal compound CaCuO_2 . The results for the energy volume variation along with the bulk modulus, electronic structure, and the den-

sity of states, and the frequencies of some frozen phonons are reported here. For the details of the LMTO method we refer to earlier papers.¹⁻³

II. CALCULATION AND RESULTS

The CaCuO_2 structure as shown in Fig. 1 has a space group $P4/mmm(D_1^{4h})$. The atomic positions in the unit cell are Cu, (0,0,0); O(1), ($a/2,0,0$); O(2), ($0,a/2,0$); Ca, ($a/2,a/2,c/2$).

For the Sr-doped sample, the experimental lattice parameters are $a=3.86 \text{ \AA}$ and $c=3.2 \text{ \AA}$ ($c/a=0.829$). The bond lengths are $\text{Cu-O}(1) = \text{Cu-O}(2) = 1.93 \text{ \AA}$ and $\text{Ca-O}(1) = \text{Ca-O}(2) = 2.50 \text{ \AA}$.

In the present calculation, the basis employed for making the expansions of the products of the LMTO envelopes included functions with $l \leq 4$ and of energies -0.01 , -1.0 , and -2.3 Ry and with decays given by $\lambda^2 = -1$ and -3 Ry . The set will include 50 functions for each atomic sphere. The local-density potential of Hedin and Lundqvist has been employed. An absolute convergence to better than 0.5 mRy/atom is obtained with spd basis of 22 LMTO's/atom for each atom including O. The number of atoms in a unit cell were taken to be four.

The muffin-tin (MT) spheres were chosen to be slightly smaller than touching and the radii for Cu, O, and Ca were taken as 2.00, 1.64, and 3.02 atomic units (a.u.), respectively. The states $\text{Cu}(3d,4s,4p)$, $\text{O}(2s,2p)$, and $\text{Ca}(3p,3d,4s)$, are taken as the valence-band electrons.

Variations both in the lattice parameter a and the ratio c/a were investigated, alternatively. The results are shown in Figs. 2 and 3, respectively. One finds an energy minimum for the volume of the unit cell $V=0.9V_0$ and $c/a=0.87$ ($c=1.02c_0$), where V_0 is the unit-cell volume for $a=3.86 \text{ \AA}$ and $c_0=3.2 \text{ \AA}$ (in fact, these lattice parameters correspond to the experimental values for the Sr-doped CaCuO_2). Thus, the calculated values are quite close to those observed for the Sr-doped material lying near 3%. The future calculations have been done for the experimental values of the parameters seen for the Sr-doped sample. The calculated value of bulk modulus of elasticity is 2.134 mbar .

The charge transfer from the muffin-tin spheres (i.e., the difference between the atomic number and the charge

CRYSTAL STRUCTURE OF CaCuO_2

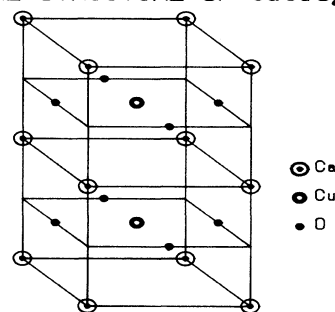


FIG. 1. Crystal structure of CaCuO_2 .

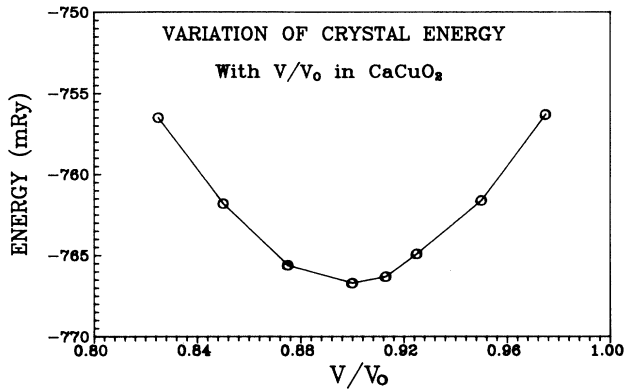


FIG. 2. Variation of crystal energy (mRy) with the ratio of unit-cell volumes, V_0 and V as described in the text.

lying within the MT sphere) of Cu, O, and Ca are 1.65, 0.56, and 0.62 electron charges, respectively. The total electron charge per unit cell outside the MT spheres is $3.39e$.

A. Electronic structure

The calculated band structure along some symmetry directions is presented in Fig. 4. The various symmetry points of the Brillouin zone are in units of $2\pi/a$ Γ , (0,0,0); X , (0.5,0,0); M , (0.5,0.5,0.6); Z , (0,0,0.6); R , (0.5,0,0.6), and A , (0.5,0.5,0.6). As the out-of-plane lattice constant c is small compared to the in-plane lattice constant a , the bands along the c direction show appreciable dispersion although it is smaller than that seen in the x - y plane (or Cu-O_2 layer).

The lowest 11 bands lying in the energy interval range of about 9 eV near and below E_F arise mainly from the Cu_{4s} , Cu_{3d} , and O_{2p} states. There is appreciable mixing with the Cu_{4s} states. This spread (≈ 9 eV) of energy bands is similar to that calculated by Mattheiss and Hamann⁸ and by Singh *et al.*⁹ using the LAPW method and by Korotin and Anisimov¹⁰ using the LMTO-ASA

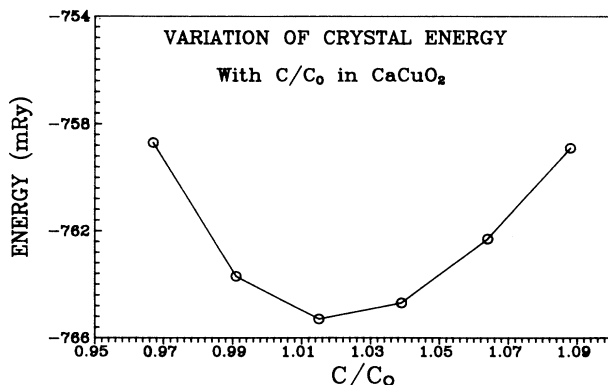


FIG. 3. Energy variation with the interlayer spacing.

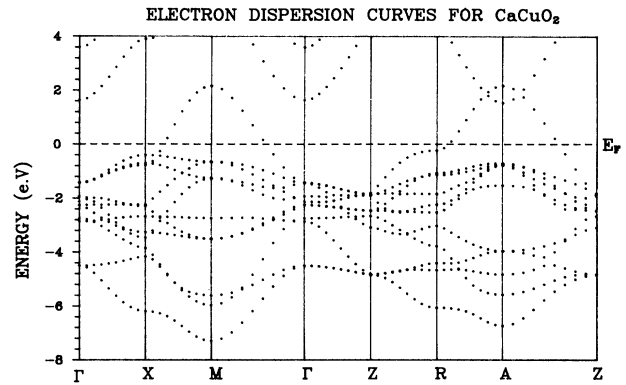


FIG. 4. Dispersion curves for the CaCuO_2 system.

method. The uppermost band crossing the Fermi level corresponds to the antibonding $\text{Cu-}d_{x^2-y^2}\text{-O-}p_{x,y}$ states.

The lower part of the Cu $4s$ bands lying above E_F overlaps the antibonding $\text{Cu-}d_{x^2-y^2}\text{-O-}p_{x,y}$ subbands near the Γ and A symmetric points.

In order to see the nature of the dispersion in another plane shifted in the c direction, we have also included in Fig. 4 the dispersion curves in the $2\pi/a$ $[0,0,0.6]$ direction.

In the calculation of the electron density of states (DOS), a tetrahedron mesh of 126 k points in the irreducible part of the Brillouin zone with a Gaussian energy broadening of 0.015 Ry was employed. The calculated DOS for the self-consistent calculation is shown in Fig. 5. The DOS shows the main features which are quite similar to those of the other oxide high- T_c cuprates.¹¹ The projected densities at various atoms have also been shown in Figs. 5(b)–5(d). At the Fermi level, the main contributions arise from the Cu($4s$), Cu($3d$), O($3p$), and Ca($3p$) states. In fact, the contribution of Cu($4s$) states dominates over the Cu($3d$) states. The Fermi level appears at the bottom of the peak lying just below it. The total density at E_F is quite small, 0.35 states/eV cell (each state can accommodate two electrons). The present density of states is overall quite similar to that of Korotin and Anisimov,¹⁰ who have employed the ASA approximation. However, the peak structures are somewhat different.

The present calculation which ignores the correlation effects predicts a metallic behavior of the system in contrast to the expected insulator-type antiferromagnetic ground state. Inclusion of the above effects lifts the spin degeneracy of the $\text{Cu-}d_{x^2-y^2}$ states opening an energy gap at the Fermi level and a nonvanishing magnetic moment.^{9,10}

The valence electron charge density for the various atoms in the two planes (001) and (0 $\bar{1}$ 1) are plotted in Figs. 6 and 7, respectively. The contours have an interval of $0.005 e/(\text{a.u.})^3$ up to a maximum of $0.15 e/(\text{a.u.})^3$.

B. Phonon frequencies

The variation of the internal energy of the solid with the various types of static deformations in the small dis-

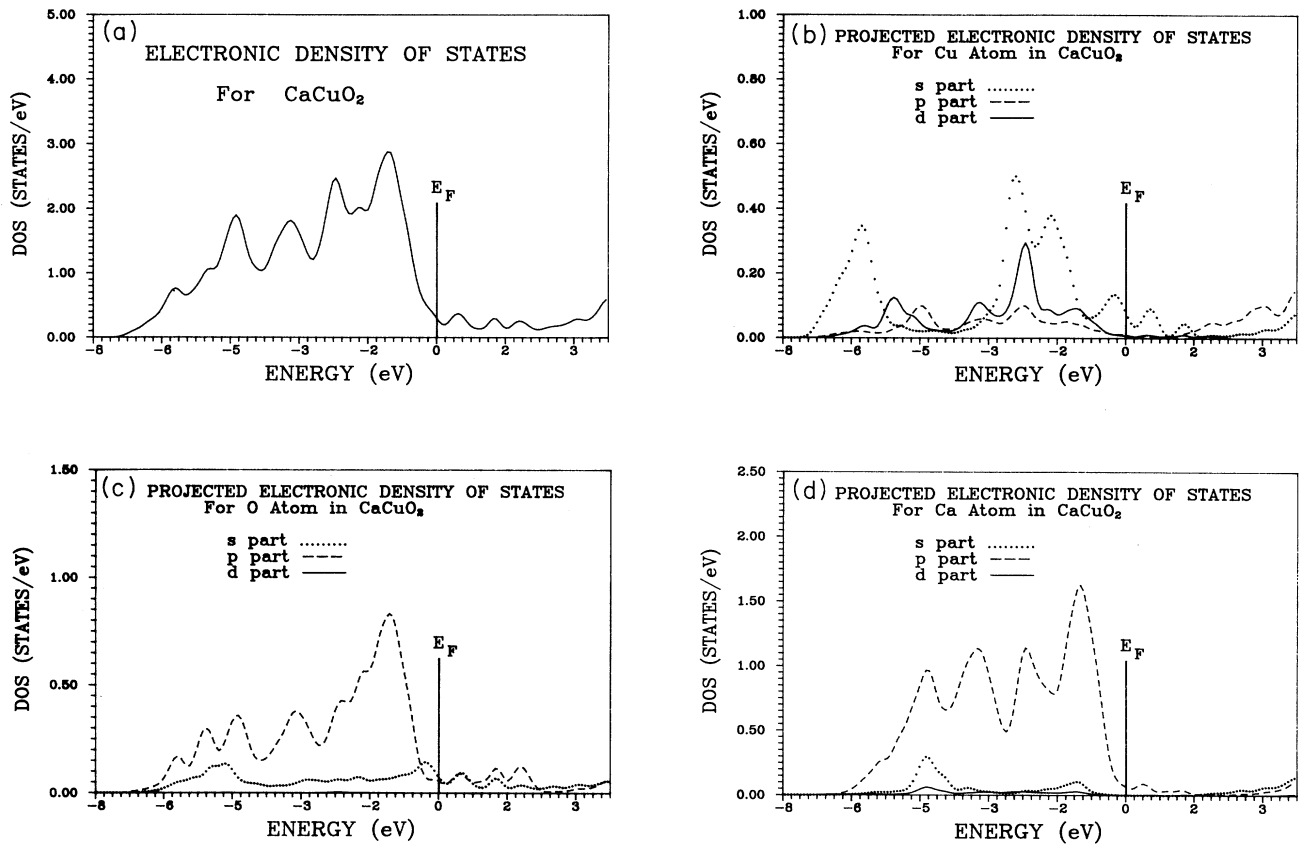


FIG. 5. (a) Total electronic density of states (DOS) for the CaCuO_2 system. (b)–(d) s , p , and d orbital contributions of the projected density of states at the Cu, O, and Ca atoms, respectively.

placement limit has been employed for calculating the frozen phonon frequencies at the $\Gamma(\mathbf{k}=0)$ point of the Brillouin zone. In CaCuO_2 , in all there are six optical modes out of which five are infrared active and the remaining sixth mode comprising of the out-of- (CuO_2) plane vibrations of oxygen atoms in opposite directions is

silent. The frequencies of these vibrations along with their eigenvectors are presented in Table I. The frequencies have been calculated by determining the harmonic force constant after fitting the energies of the distorted structure for several amplitudes with a polynomial containing terms up to third degree. In order to see the reli-

TABLE I. Frequencies of the various phonon modes ($\mathbf{k}=0$) for CaCuO_2 in cm^{-1} . The displacements of the various atoms are denoted by $\text{Cu}(X_1, Y_1, Z_1)$, $\text{Ca}(X_2, Y_2, Z_2)$, $\text{O}_1(X_3, Y_3, Z_3)$, and $\text{O}_2(X_4, Y_4, Z_4)$. The experimental frequencies in brackets are for longitudinal phonons (Ref. 12).

Sample No.	Mode symmetry	Displaced atoms	Components of displaced atoms	Cal. freq. for CaCuO_2	Exptal freq. (Ref. 12) for $\text{Ca}_{0.86}\text{Sr}_{0.14}\text{CuO}_4$
1	A_u	Cu, Ca	$(Z_1 - Z_2)$	213	186
2	A_u	O	$(Z_3 - Z_4)$	316	
3	A_u	Cu, O, Ca	$\begin{bmatrix} Z_1 + Z_2 - Z_3 \\ -Z_4 \end{bmatrix}$	422	421(440)
4	E_u	Cu, Ca	$\begin{bmatrix} X_1 - Y_1 \\ -X_2 + Y_2 \end{bmatrix}$	253	230(240)
5	E_u	Cu, O, Ca	$\begin{bmatrix} -X_1 - Y_1 \\ -X_2 - Y_2 \\ +Y_3 + X_4 \end{bmatrix}$	390	306(401)
6	E_u	Cu, O	$\begin{bmatrix} -X_1 + Y_1 \\ +X_3 - Y_4 \end{bmatrix}$	634	597(663)

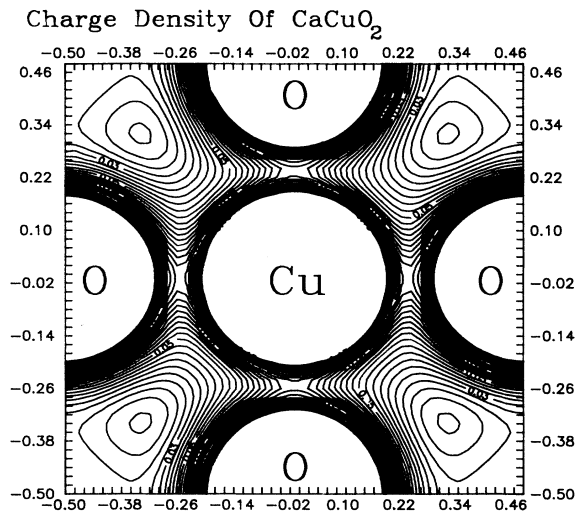


FIG. 6. Valence charge density contours in the (001) plane in the interval of $0.005 e/(\text{a.u.})^3$ up to a maximum value of $0.15 e/(\text{a.u.})^3$.

ability of the estimates of these calculated values we have also included in the table the measured values for the Sr-doped CaCuO_2 . The frequencies for the undoped sample are quite close to the observed values for the Sr-doped sample except for the E_u mode which involves the motion of all the atoms.

III. CONCLUSIONS

The LMTO method which is comparatively simple and faster than the LAPW method is able to predict one electron energy spectrum of CaCuO_2 quite similar to the LAPW method. Values for the bulk modulus and the frozen phonon frequencies have been obtained. The phonon frequencies for the undoped CaCuO_2 are quite near to those measured for the Sr-doped sample.

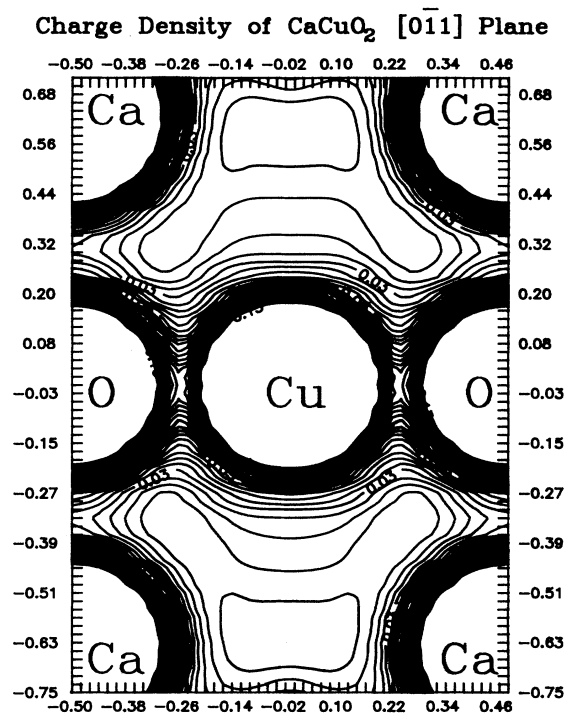


FIG. 7. Contour plots in the $(0\bar{1}1)$ plane with a key similar to Fig. 6.

ACKNOWLEDGMENTS

The authors express their sincere thanks to M. Methfessel for allowing the use of his code. All the calculations were performed on the DEIL5100 and HP720 systems available with us. Financial assistance from University Grants Commission, New Delhi, and Department of Science and Technology, New Delhi, are acknowledged.

¹M. Methfessel, Phys. Rev. B **38**, 1557 (1988).

²M. Methfessel, C. O. Rodrigue, and O. K. Anderson, Phys. Rev. B **40**, 2009 (1989).

³Bal K. Agrawal and Savitri Agrawal, Phys. Rev. B **45**, 8321 (1992).

⁴M. Methfessel, Bal K. Agrawal, and M. Scheffler (unpublished).

⁵C. C. Toradi *et al.*, Science **240**, 631 (1988).

⁶T. Siegrist, S. M. Zahurk, D. W. Murphy, D. W. Roth, and R. S. Roth, Nature **334**, 193 (1988).

⁷X. Smith *et al.*, Nature **351**, 549 (1991).

⁸L. F. Mattheiss and D. R. Hamann, Phys. Rev. B **40**, 2717 (1989).

⁹D. Singh, W. E. Pickett, and H. Krakauer, Physica C **162-164**, 1431 (1989).

¹⁰M. A. Korotin and V. I. Anisimov, Mater. Lett. **10**, 28 (1990).

¹¹W. E. Pickett, Rev. Mod. Phys. **61**, 433 (1989).

¹²G. Burns *et al.*, Phys. Rev. B **40**, 6717 (1989).